# REPORT DOCUMENTATION PAGE

Public Reporting burden for this collection of information is estimated to average 1 hour per response, including the time for reviewing instructions, searching existing data sources, gathering and maintaining the data needed, and completing and reviewing the collection of information. Send comment regarding this burden estimates or any other aspect of this collection of information, including suggestions for reducing this burden, to Washington Headquarters Services, Directorate for information Operations and Reports, 1215 Jefferson Davis Highway, Suite 1204, Arlington, VA 22202-4302, and to the Office of Management and Budget, Paperwork Reduction Project (0704-0188,) Washington, DC 20503.

| 1. AGENCY USE ONLY ( Leave Blank) | 2. REPORT DATE June 07, 2004 | 3. REPORT TYPE AND DATES COVERED Final Report; from 7/01/02 to12/31/03 |
|---|---|---|

**4. TITLE AND SUBTITLE**

Hydrogen in Bulk metallic Glasses: Storage Potential and Effects on Structure

**5. FUNDING NUMBERS**

DAAD19-02-1-0277

**6. AUTHOR(S)**
K.S. Kumar and P. Wang

**7. PERFORMING ORGANIZATION NAME(S) AND ADDRESS(ES)**

Brown University, Providence, Rhode Island 02912

**8. PERFORMING ORGANIZATION REPORT NUMBER**
None

**9. SPONSORING / MONITORING AGENCY NAME(S) AND ADDRESS(ES)**

U. S. Army Research Office
P.O. Box 12211
Research Triangle Park, NC 27709-2211

**10. SPONSORING / MONITORING AGENCY REPORT NUMBER**

44256.1-MS

**11. SUPPLEMENTARY NOTES**
The views, opinions and/or findings contained in this report are those of the author(s) and should not be construed as an official Department of the Army position, policy or decision, unless so designated by other documentation.

| 12 a. DISTRIBUTION / AVAILABILITY STATEMENT | 12 b. DISTRIBUTION CODE |
|---|---|
| Approved for public release;  distribution unlimited. | |

**13. ABSTRACT (Maximum 200 words)**

Several new ferrous and no-ferrous compositions that are capable of forming metallic glasses in bulk form have been examined for their potential to reversibly ingest hydrogen and discharge it. Hydrogen charging was done both by gas charging at pressure and temperature and by the electrochemical route. Results from both approaches were in good agreement and showed that the Fe-based and Y-based glasses were not capable of ingesting hydrogen whereas the Zr-based and Cu-based glasses could take in an appreciable amount of hydrogen but were incapable of discharging it. The hydrogen in the latter alloys interfered with the crystallization process upon heating. The residual hydrogen in the material however served as a qualitative probe for determining possible structural variations in the glass from the inside to the outside. Specifically, calorimetric scans of hydrogen-charged specimens extracted from the center of the ingot were visibly different from those obtained from the edge, suggesting that the structure was more relaxed in the central portion of the ingot. Calorimetric scans of the Zr-based glass at various rates from 0.1°C/min to 100°C/min confirmed a strong heating rate dependence of the glass transition temperature and the crystallization response, the effect being more dramatic in the 0.1°C/min-10°C/min regime.

**14. SUBJECT TERMS**
Hydrogen, Bulk Metallic Glass, Differential Scanning Calorimetry, glass transition temperature, crystallization, hydrogen storage, hydrogen discharge

**15. NUMBER OF PAGES**
28

**16. PRICE CODE**

| 17. SECURITY CLASSIFICATION OR REPORT UNCLASSIFIED | 18. SECURITY CLASSIFICATION ON THIS PAGE UNCLASSIFIED | 19. SECURITY CLASSIFICATION OF ABSTRACT UNCLASSIFIED | 20. LIMITATION OF ABSTRACT UL |
|---|---|---|---|

# 1.0    Table of Contents

## 2.0    Statement of the Problem Studied

New bulk metallic glass (BMG) compositions are continuously being identified and cast using conventional methods to reasonable sizes (for example > 5 mm diameter). These include alloys in the Fe-based system, Al-based system, Y-based systems, Ni and Cu-based systems, and refractory metals-based system in an on-going research effort at the California Institute of Technology (Professor Bill Johnson) and University of Virginia (Profs. Gary Shiflet and Joe Poon) and sponsored by the Defense Advanced Research Projects Agency (DARPA).  Our goal was to examine these new alloy systems for their hydrogen storage potential and to understand the consequence of hydrogen presence on the transformation response of the alloy.

Specifically, in the proposed <u>one-year</u> program, we had decided to address the following issues:

1)    Identify the maximum solubility of electrochemically charged hydrogen at room temperature and at 70°C at ambient pressure in Fe-based, Al-based, and refractory-metal based amorphous alloys, and how alloy composition affected this solubility limit?

2)    Understand the ease of hydrogen desorption electrochemically – i.e. can we discharge hydrogen electrochemically from such a glass at near-ambient temperatures and pressures?

3)    Examine the effect of a surface film on the desorption kinetics.

4)    Determine the effect of absorbed hydrogen on the stability of the amorphous material – i.e. how does hydrogen intake affect the glass transition and crystallization temperatures?

While the scope of this one-year effort would not realistically permit us to go beyond the characterization phase, the findings would most likely enable us to "design" and recommend compositions for metallic glasses that are directed to hydrogen storage applications.

# 3.0    Technical Background

Hydrogen is a powerful, clean, synthetic fuel with the inconvenient property of being an ideal gas at ambient temperature and pressure.  In order to use hydrogen efficiently as a fuel, it has to be compacted for mobile storage and this is a non-trivial issue.  Different methods of storage range from classical methods such as using high pressure or liquefaction to sorption on high surface area solids or bulk sorption, to newer chemical processes that suffer from the lack of reversibility.  None of the present solutions is economically competitive yet with today's inexpensive liquid hydrocarbons [1].  However, as the search continues for the non-$CO_2$ producing options, we need to compare the hydrogen solution with other alternatives.  The problem with storage of hydrogen in high-pressure hydrogen tanks is that they deliver hydrogen at varying pressures; liquefaction of hydrogen results in high energy losses.

Metallic systems (metals, alloys and intermetallic compounds) interact with hydrogen to form hydrides.  These materials (particularly intermetallics) have attracted considerable attention because of their potential to serve as media for hydrogen storage. In the late 1960s it was discovered that certain intermetallic compounds ($Mg_2Ni$, $LaNi_5$ and TiFe) would directly and reversibly react with hydrogen gas at temperatures in the range 250-650K.  These observations coupled with the energy crisis in the 1970s stimulated extensive investigations of metal hydrides for energy storage and conversion. Hundreds of intermetallic alloys have been screened for hydrogen-storage potential. Metal hydrides may be formed through gas-phase absorption or via an electrochemical process.  Gas-phase applications include stationary fuel storage, vehicular fuel storage, chemical heat pumps and refrigerators and for sorption coolers for space flight applications while metal hydrides are also used in electrochemical energy-storage cells (Over the past decade, Ni-metal hydride (MH) batteries have displayed their ability to replace Ni-Cd batteries in a variety of application).  Important considerations in the selection of a system [2] include: 1) how easily hydrides are formed and decomposed (thermodynamics and kinetics), 2) heat of decomposition of the hydride, 3) the maximum amount of hydrogen that can be absorbed, 4) chemical and physical stability of the storage medium, 5) cost, 6) weight and 7) safety issues. The hydrogen storage capacity in metals and alloys is determined by chemical interactions between the metal and hydrogen atoms, as well as by the type, number and size of the potential interstitial sites for hydrogen.  In most materials, hydrogen tends to occupy tetrahedral interstitial sites.  A recent comprehensive review of the subject [3] and several overview articles in the September 2002 issue of the *MRS Bulletin* [4] provide a detailed discussion of current trends in the hydrogen-storage alloy-development arena.

Prior research efforts on amorphous ribbons and wires have shown that hydrogen solubility in the amorphous state can be substantial and that charging and discharging can be a *reversible* phenomenon [5-17] depending on the composition of the glass.  Further, it

was also claimed [7] that unlike the intermetallic compounds $LaNi_5$ and FeTi that disintegrate when hydrogen-charged ($LaNi_5$ shows a volume expansion of 25% upon the absorption of hydrogen), metallic glasses can be embrittled by hydrogen but they do not disintegrate readily.  Studies on Zr-based glasses in ribbon form have shown that:

• For a binary amorphous Ni-Zr alloy with the stoichiometry $Ni_{1-x}Zr_x$, where x varies from 0 to 1, the H/M increases as x increases – i.e. as the Zr fraction in the alloy increases [18].

•  A partially quasicrystalline Zr-Cu-Ni-Al alloy (the rest being glassy) exhibits a higher H/M and faster charging kinetics than a completely glassy material.  The H/M for the partially crystalline material is = 2.0.  Furthermore, a Pd film coating significantly enhances the charging kinetics [19].

• The composition of the glass within a family of alloys (e.g. Zr-based) significantly influences the amount of hydrogen that can be ingested in the material.  For example, it has been shown that a $Zr_{75}Fe_{25}$ glass saturates at an H/M = 1.0 whereas a comparable alloy of composition $Zr_{75}Pd_{25}$ saturates at H/M = 1.75 in half the time [5].

•  Hydrogen discharge from a glass with the composition $Zr_{69.5}Cu_{12}Ni_{11}Al_{7.5}$ is sluggish and does not occur till the specimen is heated to temperatures in excess of 500°C in ultra-high vacuum [20].  At these temperatures, crystallization of the glass also occurs and thus the glassy state is lost.  This difficulty has been attributed to the formation of a zirconium oxide barrier.

• Recently, results from a study of a Zr-based glass [21] with a composition corresponding to one that is capable of being produced in bulk form ($Zr_{55}Al_{10}Ni_5Cu_{30}$) and one that exhibits a large temperature region between the glass transition temperature and the crystallization temperature confirmed the presence of a plateau in the P-C isotherm (PCT diagram as it relates to Sieverts law and gas-charging of hydrogen) comprising a hydrogen concentration range from 0.7 to 1.4 mass percent hydrogen at 573K and a hydrogen pressure of 1.8 MPa.  The existence of the plateau was ascribed to the formation of an amorphous hydride.

More recently, Mg-Ni alloys have been the focus of research for hydrogen storage application and a recent overview of the subject by Schwartz [22] summarizes the salient aspects of the findings thus far.  Since Mg-based alloys are difficult to melt typically, mechanical alloying has been the preferred route to producing nanocrystalline and amorphous alloys.  Alloys thus produced have been shown to possess lower absorption/desorption temperatures than conventionally crystallized alloys and indicate the possibility of electrochemical absorption and desorption at room temperature. Yamaura et al [23] have also produced a ternary $Mg_{67}Ni_{28}Pd_5$ amorphous alloy by melt spinning and have examined the hydrogen absorption and desorption capability of this alloy.  They found that the principal difference was that the discharge capacity increased with increasing the number of charge/discharge cycles in contrast to mechanically

alloyed Mg-Ni amorphous alloys.  The maximum discharge capacity was after 25 cycles at 308K and was 411 mAh/g.  Interestingly, the discharge capacity decreased with increasing current density.  They also noted that hydrogen stabilized the amorphous phase.

New bulk metallic glass compositions are continuously being identified in Fe-based systems of the type Fe-Cr-Mo-C-B-P [24], Fe-Co-Ln-B [25], Fe-(Al,Ga)-(P, C, B, Si, Ge) [25] and Fe-(Zr, Hf, Nb)-B [25].  Amorphous ribbons of new compositions have been developed in the Al-based systems (for example: 75Al-17Cu-8Mg with 2-8% Ni addition in ref. [26]).  These metallic glasses with low levels or no refractory metals may discharge hydrogen more readily than do the Zr-based bulk metallic glasses.

The purpose of this study (and a related previous effort [27]) is to examine the hydrogen storage potential of these new bulk metallic glasses.  Whereas the previous effort was primarily focused on a Zr-based bulk metallic glass, this effort included several newer compositions not based on the Zr system.  For purposes of continuity however, results from the previous effort are summarized in the next section and for reasons discussed in the next section, further experiments were also conducted in this study on the Zr-based alloy.

## 4.0    Highlights of the Previous Effort

In a previously concluded one-year exploratory effort [27], we examined the hydrogen storage potential of a Zr-based bulk metallic glass (Zr-18Cu-15Ni-5Ti-10Al in at.%).   The material was provided by Dr. C.T. Liu of Oak Ridge National Laboratory. We found that electrochemically, it is possible to incorporate hydrogen into the material at ambient temperature and pressure to the extent of H/M = 1.5 (H/M = hydrogen to metal ratio) before any fracture occurred.  The kinetics of hydrogen absorption was significantly affected by the temperature at which hydrogen is electrochemically charged. The development of cracks in the material after hydrogen charging was recorded, and demonstrated a pattern consistent with strain induced due to hydrogen absorption. The crack always initiated at the circumference and ran radially inwards for a short distance before reorienting itself into a path that is concentric with the circumference.  This was argued to be a consequence of the volume expansion resulting from the hydrogen ingestion.  Measured radial strains indicate values of the order of 2-3 percent prior to failure.  The effects of current density on charging kinetics as well as a comparison of charging in an acid solution versus a base solution for a fixed specimen thickness were documented.  An H/M =1.5 was achieved in the KOH solution before the first crack appeared in the specimen.

The above observations pertain to hydrogen absorption capacity and related kinetics and the structural integrity of the candidate material.  Of equal importance is the ability for the material to discharge the hydrogen relatively easily.  Results from a recent paper [28] confirm that hydrogen discharge from a glass with the composition $Zr_{69.5}Cu_{12}Ni_{11}Al_{7.5}$ is sluggish and does not occur till the specimen is heated to temperatures in excess of 500°C in ultra-high vacuum.  At these temperatures, crystallization of the glass also occurs and thus the glassy state is lost.  This difficulty has been attributed to the formation of a zirconium oxide barrier.  Attempts to lower the hydrogen discharge temperature by depositing a Pd layer that would inhibit oxide formation, or alternately modifying the alloy composition with Pd additions have been only partially successful.

Similar observations were also made in our recent effort. Discharging the electrochemically charged hydrogen proved to be a futile task.  Hydrogen-charged specimens were annealed in air and in diffusion pump vacuum at room temperature, 70°C, 300°C and at 425°C.  The last of these temperatures is above the glass transition temperature of the alloy but below the crystallization temperature.  After annealing the specimen charged to an H/M = 1.46 at 300°C for 2h in a diffusion pump vacuum, a measurable weight loss was registered and interpreted as being hydrogen desorption.  The H/M of the material reduced to 1.285; further annealing of the specimen at 425°C for 2h

resulted in virtually no reduction in H/M (H/M = 1.26) and whether this was a consequence of surface oxide barrier from the previous thermal exposure (surface polishing was not possible due to the warped surface profile) or due to strongly-bound hydrogen in the tetrahedral sites in the glass remains to be verified.

Annealing the hydrogen-charged material in air in a DSC cell however illustrated that the hydrogen in the material affected the crystallization process in a reproducible way. The as-received material (as-cast condition) prior to any hydrogen charging (H/M = 0) exhibits a Tg of ~404°C (Figure 1) and a double peak during crystallization. The first of these two peaks is interpreted as a phase separation peak [29] in such Zr-based glasses (amorphous phase + nanocrystalline phase), and the second major peak corresponds to the devitrification of the remaining amorphous material.
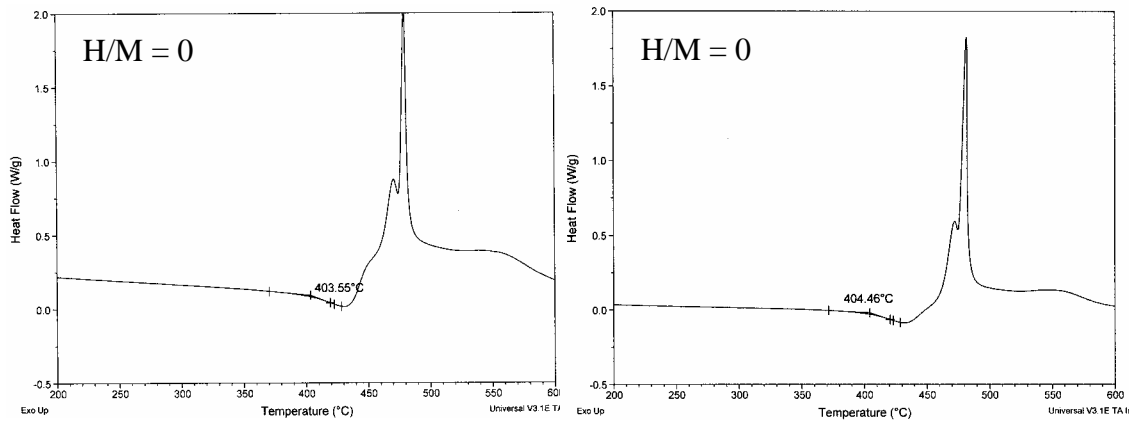


**Figure 1**: Reproducible DSC scans of the as-received Zr-based bulk metallic glass (H/M = 0; 52.5Zr-17.9Cu-14.6Ni-5.0Ti-10.0Al) illustrating a glass transition temperature of ~404°C and a double peak during crystallization.

The corresponding DSC scans for the material containing hydrogen (H/M = 0.83) are shown in duplicate in Figure 2. Clearly, the results are reproducible. It is noted that the presence of hydrogen affects the glass transition temperature and the crystallization process. Specifically, the glass transition temperature is lowered by ~15°C and the "double peak" during crystallization is no longer recognized; the phase separation peak appears to have been suppressed. This latter response was also noted in [29] for a similar Zr-based glass. However, there is disagreement with respect to the effect of hydrogen on the glass transition temperature.
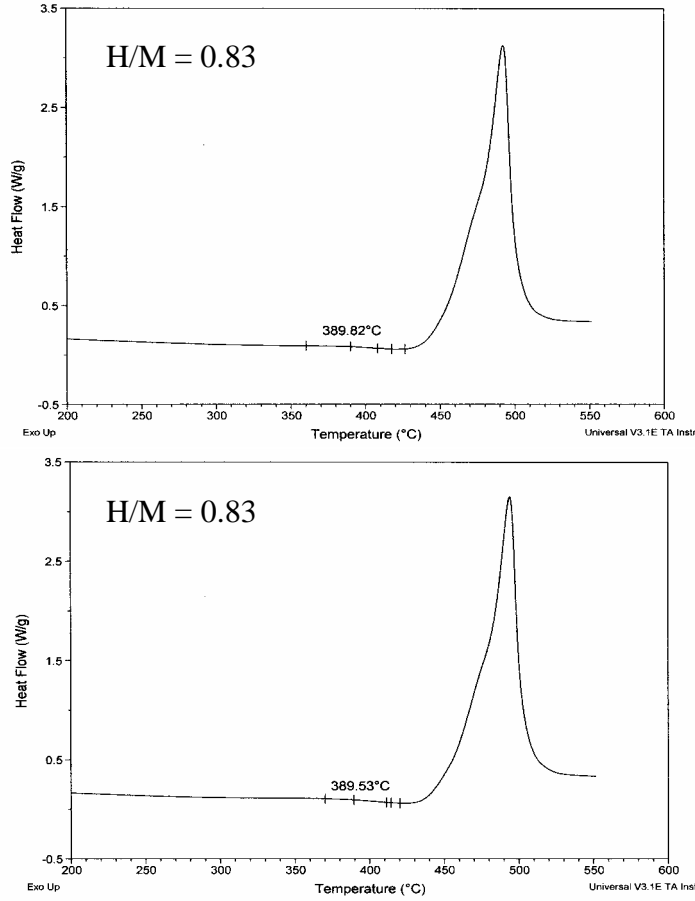
7

**Figure 2**. Reproducible DSC scans of the hydrogen-charged (H/M = 0.83) Zr-based bulk metallic glass illustrating a glass transition temperature of ~390°C and a broad single peak during crystallization.

Ismail et al [30] conducted a detailed and systematic study on the effect of hydrogen on the devitrification process in a Zr-based glass ($Zr_{65}Cu_{17.5}Al_{7.5}Ni_{10}$) and noted that the response depended on the level of hydrogen in the alloy. Prior toany hydrogen charging, this alloy has a glass transition temperature of 643K and crystallization occurs at 740K with the formation of a quasicrystalline phase. When hydrogen is charged in this alloy (up to H/M = 0.4), it was found that the formation of the quasicrystalline phase was suppressed and instead Cu clustering was encouraged and nanocrystals of Cu and Cu-rich phases formed. At H/M = 0.7, a glass transition temperature was no longer evident; $\varepsilon$-$ZrH_2$ was observed as the first phase upon crystallization followed by $\delta$-$ZrH_2$ and then, nanocrystalline Cu. Furthermore, the $\delta$-$ZrH_2$ transformed to $\alpha + \beta$-ZrH. At the very high H/M level of 1.6, hydrogen desorption commenced at 433K from those sites with lower affinity to hydrogen; at 598K, $\varepsilon$-$ZrH_2$ formed and decomposed at higher temperatures and transformed to $\delta$-$ZrH_2$. The stripping of all the Zr from the alloy was found to lead to the

precipitation of new nanocrystalline C-rich phases. Clearly, hydrogen in the alloy significantly influences microstructure evolution upon devitrification.

New BMG compositions are continuously being identified and cast using conventional methods to reasonable sizes (for example > 5 mm diameter). These include alloys in the Fe-based system, Al-based system, Y-based systems, Ni and Cu-based systems, and refractory metals-based system in an on-going research effort at the California Institute of Technology (Professor Bill Johnson) and University of Virginia (Profs. Gary Shiflet and Joe Poon) and sponsored by the Defense Advanced Research Projects Agency (DARPA). Our proposal was to examine these new alloy systems for their hydrogen storage potential and to understand the consequence of hydrogen presence on the transformation response of the alloy. A principal attractive driver is that the ease of hydrogen discharge is intimately tied to the strength of the metal-hydrogen bond. Whereas this bond is strong in the Zr-based system, it is likely to be less strong in these Ni-based, Cu-based and Fe-based systems and thus these materials may have a higher potential for use as a hydrogen storage material.

## 5.0      Summary of Experimental Results

### 4.1     *Materials and Initial Characterization*

Five different alloy compositions were examined. Their composition and molar weights are provided in Table I. Whereas BMG1 was the previously examined material included for purposes of comparison, BMG2 and BMG4 were provided by Prof. Johnson at the California Institute of Technology and BMG3 and BMG5 were provided by Prof. Poon at the University of Virginia. Three materials were obtained late in the Fall of 2002 and BMG5 was obtained in the summer of 2003. BMG2 and BMG4 were in plate form whereas BMG3 were rods about 1-2 mm in diameter and about 15 mm long and BMG5 was a small irregular piece from a casting. Note that BMG2 is fairly similar in composition to BMG1 with Ti being replaced by a similar level of Nb; BMG4 was porous and contained cavities that appeared to be gas pores. Further, although a nominal composition is listed for BMG3, the actual pieces were really "scrap pieces" from a range of compositions, and hence a range is provided in Table I for the Fe content. All four materials (BMG2-BMG5) were made available only in small quantities. While awaiting these materials, detailed characterization effort was continued on BMG1, the only one of the five materials listed in Table I that was available in adequate quantities and geometry suitable for systematic experimental purposes.

| Sample # | Composition (at. %) | Molar Weight |
|---|---|---|
| BMG1 (ORNL) | Zr (52.5)-Cu (17.9)-Ni (14.6)-Ti (5.0)-Al (10.0) | 72.928 g |
| BMG2 (Vitreloy 106) | Zr (57)-Cu (15.4)-Ni(12.6)-Nb (5.0)-Al (10.0) | 76.52 g |
| BMG3 (U of Va) | Fe (54-55)-Mn (10)-Cr (4)-Mo (10)-C (15)-B (6-7) | 50.11 g |
| BMG4 (Vitreloy 101) | Cu (47)-Ti (34)-Zr (11)-Ni (8) | 60.881 g |
| BMG5 (U of Va) | Actual composition not provided-"told Y-based" | |

The as-received alloys were characterized using X-ray diffraction to confirm they were amorphous, and then thermally scanned using differential scanning calorimetry (DSC) to determine the glass transition temperature, $T_g$, and the crystallization temperature $T_x$. The response of BMG1 was shown in Figure 1. The DSC result for BMG2 is shown in Figure 2. The scan was reproducible and displays a glass transition temperature of ~414°C and a double crystallization peak commencing at ~476°C; these features are very similar to those observed in Figure 1 for BMG1 and not surprisingly since both these alloys belong to the Zr-based family of bulk metallic glasses with some

compositional differences that are reflected in the actual transition temperatures.  As mentioned before, the double peak in the crystallization process is indicative of primary phase separation and subsequent crystallization of the amorphous matrix.
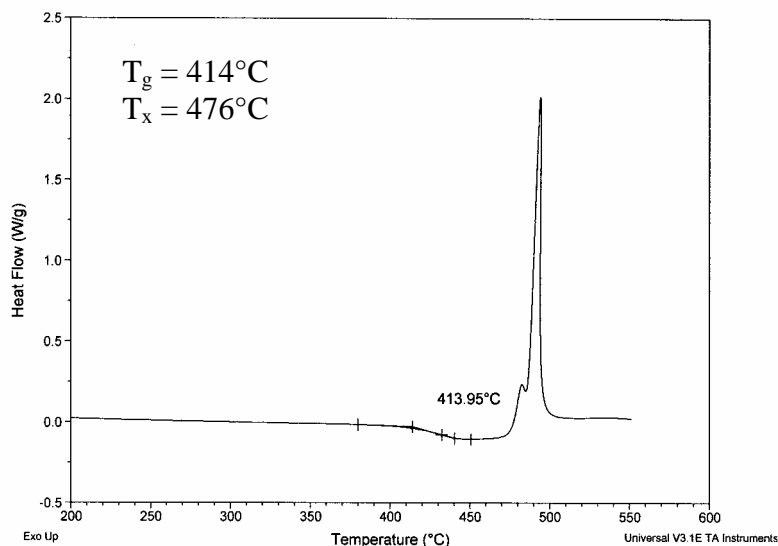


$T_g = 414°C$
$T_x = 476°C$

413.95°C

**Figure 3**:  A DSC scan for BMG2 in the as-received condition showing a distinct glass transition temperature and a double-peak crystallization response.
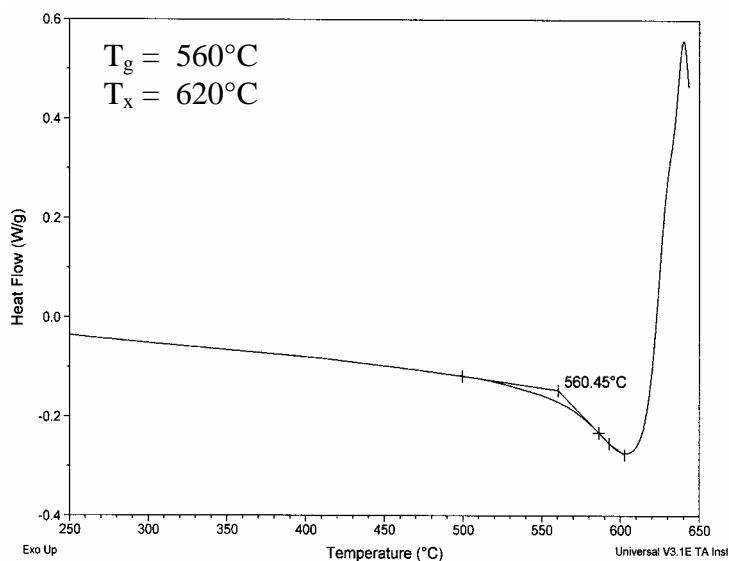


$T_g = 560°C$
$T_x = 620°C$

560.45°C

**Figure 4**:  A DSC scan for BMG3 in the as-received condition showing a glass transition temperature and a single peak crystallization response.

The DSC scan for BMG3 is displayed in Figure 4.  The glass transition temperature is 560°C and is significantly higher than for BMG1 and BMG2.  The $\Delta T$ between glass transition and crystallization is about 60°C which compares well with BMG1 and BMG2.  Crystallization is appraently not a two-step process in BMG3 as only a distinct single peak is observed in Figure 4.

In the case of BMG4, the DSC scans were reproducible but the glass transition temperature and crystallization temperature were not readily delineated. In the literature, the Tg and Tx for this alloy is reported as 398°C and 444°C and the alloy is reported to decompose prior to crystallization into copper-enriched and Ti-enriched regions [31,32]; furthermore, the presence of small quantities of Si in the alloy has been claimed to affect these temperatures [33]. A typical DSC scan for BMG4 is shown in Figure 5 (five different specimens of this material were scanned and the data shown below was reproducible). The profile observed does not match anything reported in the literature leading to the question whether what we have as BMG4 is indeed what the composition reported in Table I is, or if it is some other alloy. The DSC profile reported in literature for 47Cu-34Ti-11Zr-8Ni is very different from what is shown below. Since we received a very small piece of this material, we have not had the opportunity thus far to perform composition analysis.
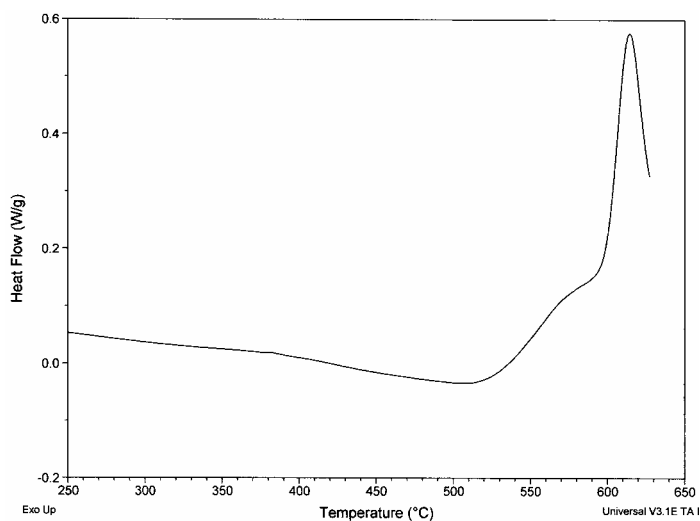


**Figure 5**: A DSC scan for BMG4 showing a possible glass transition temperature of around 380°C but then a long temperature regime with no transformation till a temperature of over 500°C before an upward swing of the curve.

Differential scanning calorimetry scans at heating rates of 10°C/minute and 20°C/minute are shown for BMG5 in Figures 6a,b. The doubling of the heating rate leads to a marginal increase in the glass transition temperature from 362°C to 367°C and similar shifts in the crystallization temperatures (compare Figure 6a and 6b).
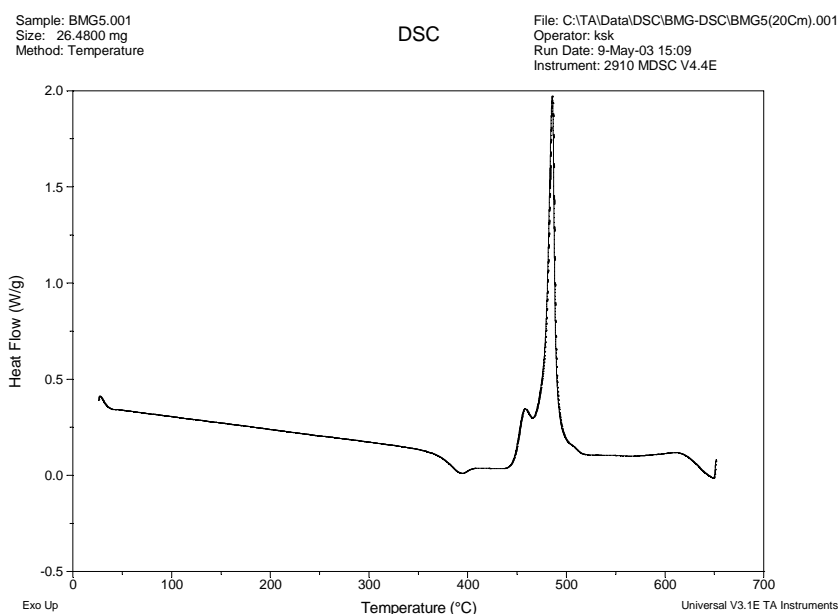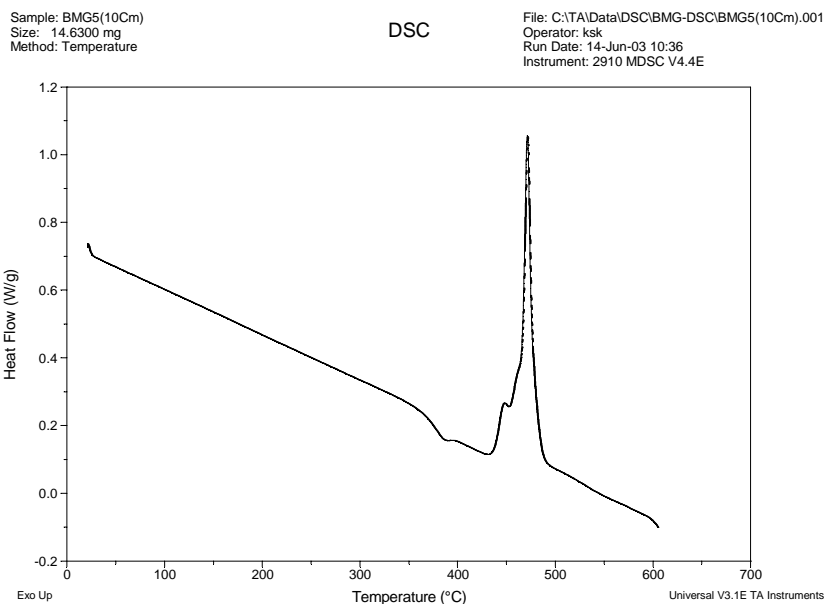
12

Figure 6: DSC scans for BMG5: (a) 10°C/minute and (b) 20°C/minute.

## 4.2 *Electrochemical Hydrogen Charging of BMG2-5*

Electrochemical hydrogen charging experiments using acid and base solutions were performed on all four alloys (BMG2, BMG3, BMG4 and BMG5) at room temperature in a manner similar to that previously done for BMG1 [27]. The acid solution used was of 0.5N $H_2SO_4$ (sulfuric acid) and the base solution was 0.25M or 0.5M KOH (potassium hydroxide). All materials showed signs of degradation before H/M could reach 0.04 for charging times ranging from 1 to 72 hours. This is in contrast to BMG1 which could

routinely be charged to H/M = 0.8-0.9, and on one occasion, to H/M = 1.46 before first fracture occurred.

Specific tests and outcomes are presented below for each alloy.

**BMG2**:

- 0.25M KOH, 100 mA, 3 hr -- the sample fractured.
- 0.25M KOH, 50 mA, 4 hr – the sample fractured.
- 0.25M KOH, 50 mA, 3 hr –repeat test (H/M was 0.109) and when this was continued for another 7 hours there was no further change in the H/M ratio.
- When the testing conditions were modified  and the electrolyte was changed to 0.5N $H_2SO_4$, and charging was accomplished at a current of 50mA for 38 hr (7+7+24) the H/M was 0.04 and on continued charging for another 24 hours the sample fractured.

**BMG3:**

- 0.25M KOH, at 100 mA, for 3 hr the H/M was 0.04. When the current was decreased to 50mA and charging carried out for another 4 hours, the sample began fragmenting and a weight loss was recorded. Charging was nevertheless continued for 6 more hours and a weight gain was recorded. Another 6 hours of charging caused the sample to break and a weight loss was recorded.  This phenomenon of weight gain followed by fragmenting and associated weight loss and then some weight gain again and the entire cycle repeating itself was a common occurrence for BMG3.

**BMG4:**

- 0.5N $H_2SO_4$ at 100 mA for 1 hr -- sample fractured. When tested in the same electrolyte at 50mA for 1 hour, once again the sample fractured.

- 0.5M KOH at 100 mA and 50 mA for 1 hr -- the sample fractured.

This frequent fracturing of the specimen precluded meaningful tests from being conducted as the experiments rely on gravimetric analyses.  Thus alternate approaches were investigated.

The first approach was to use a platinum cup to contain the BMG alloys with the idea that fracture of the piece during charging would not cause material loss if it was contained, and a platinum cup was chosen because it was assumed and subsequently proven that platinum does not ingest hydrogen and thus, all measured weight gain could be attributed to the specimen ingesting hydrogen.  However, after several trials, we

recognized other problems that came along with this approach including the difficulties associated with washing the contents of the platinum cup after each increment of time prior to measuring the weight gain, as well as difficulties associated with drying the contents (it is pertinent to recognize that weight gains or lack thereof are being measured on the microgram scale). For the latter purpose, a desiccator with a mechanical pump attachment was set up and was reasonably successful. The bigger problem however was the inability to contain the very fine fragmented particles from the specimen that attached themselves to the hydrogen bubbles resulting from recombination at the cathode, rising to the surface, and often being lost. This once again caused difficulties in accurate weight gain measurements being made. After several unsuccessful attempts at refining this method, it was abandoned.

Next, we attempted to pulverize the BMG alloys, blend them with copper powder and cold press them into a high-density compact disk about 1 cm in diameter and 1 mm thick. Hydrogen charging was carried out using the composite disk as the cathode. A reference compacted copper disk was also similarly charged as was a fully-dense, wrought copper disk of similar dimensions, machined from a copper rod. Whereas, the full-density copper disk showed no weight increase after several hours of charging in a base solution (the copper was attacked in the acid solution), the powder-processed copper disk and the composite disk showed continuous weight increase with charging time. The powder processed copper disk did not plateau off in weight gain with time and this once more made it impossible to obtain the fractional weight gain attributable to hydrogen in the composite disk. The porosity in the copper disk is thought to be the source of the problem. Attempts to dry the solution out of the pores using a vacuum system were not successful—it is believe that base residue (KOH) was still left in the pores and the resulting weight gain varied from compact to compact.

These experimental challenges made it very difficult to conduct gravimetric measurements for hydrogen in these materials using the electrochemical approach. At this stage, it was deemed necessary to attempt gas-charging these specimens to examine hydrogen storage capabilities of these metallic glasses. Gas charging requires a Sievert's apparatus that we do not have at Brown University. We however located one such piece of equipment at HRL Laboratories in Malibu, CA and Dr. John Vajo from HRL has conducted a few experiments on our behalf, free of charge, during the period June 2003 to December 2003. We sent him samples of four alloys listed in Table I (BMG1-BMG4), and the experimental details and results from his studies are presented in this report. Since the electrochemical charging experiments at Brown on BMG2-5 did not provide encouraging results, we took the approach of characterizing uncharged and hydrogen-charged BMG1 in greater detail with the intentions of better understanding hydrogen interaction with the amorphous structure. These findings are reported in the next section. The initial microstructural characterization and hydrogen charging results from

15

electrochemical charging of BMG1 were summarized in a previous report [1] and therefore are not repeated here in their entirety but are either referenced or if relevant reproduced where necessary for completeness of this report.

*4.3    Further Characterization of **BMG1*** (52.5Zr-17.9Cu-14.6Ni-5.0Ti-10.0Al)

The microstructure of the as-received BMG1 was examined in the TEM to determine whether the material was truly amorphous across the entire cross section since the crack growth pattern observed upon hydrogen charging was rather curious [27]. Optical examination of the cross section of the cylindrical cast specimen often indicated a faint "swirl" pattern whose origin appeared to reside in the freezing behavior of the alloy but whose identity remained undetermined. It was decided that the microstructure would be examined at significantly higher magnifications (than possible using metallography) in the TEM. A TEM jet-polished sample surface is shown in Figure 7a and parallel rows of fine precipitate-like features are observed running diagonally across an otherwise featureless matrix. The jet-polished perforation is seen at the bottom left corner of the micrograph in dark contrast. One row of "precipitates" can be seen running to the edge of the perforation offering the potential for a few of the precipitates to be present in the electron-transparent region of the foil. A higher magnification image of two of these precipitates can be seen in Figure 7b and it is evident that these precipitates are crystalline and faceted. Diffraction patterns obtained from the matrix and the precipitate are provided in Figures 7c and 7d respectively. Whereas the matrix is amorphous, these coarse precipitates provide diffraction patterns that are suggestive of their single crystalline nature; this is in contrast to the observation of differential contrast in the precipitate in the upper left side of Figure 7b that illustrates what could be a grain or sub-grain boundary.
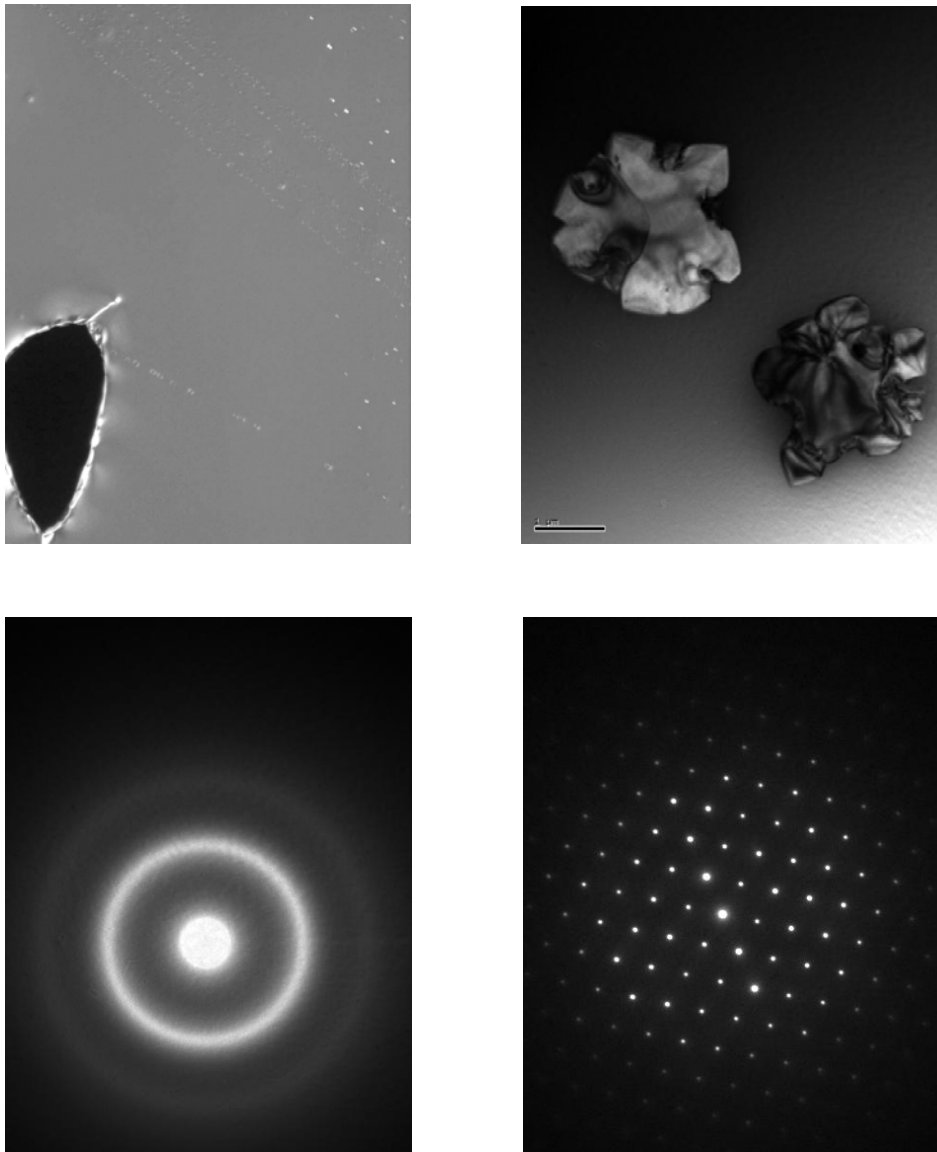
**Figure 7a-d**: Transmission electron microscopy examination of the microstructure of BMG1 confirms the presence of some coarse crystalline particles in an amorphous matrix. In (a) a low magnification optical micrograph taken in the vicinity of the perforation in the TEM specimen confirms the presence of rows of fine particles that are demonstrated to be faceted crystalline second phase particles in (b). Selected area diffraction confirms the matrix to be amorphous (c) and the particles to be crystalline (d).

We next examined the effect of heating rate on the glass transition temperature and the crystallization response of BMG 1 over a wide range of heating rates. These results are summarized in Figures 8a,b and 9.
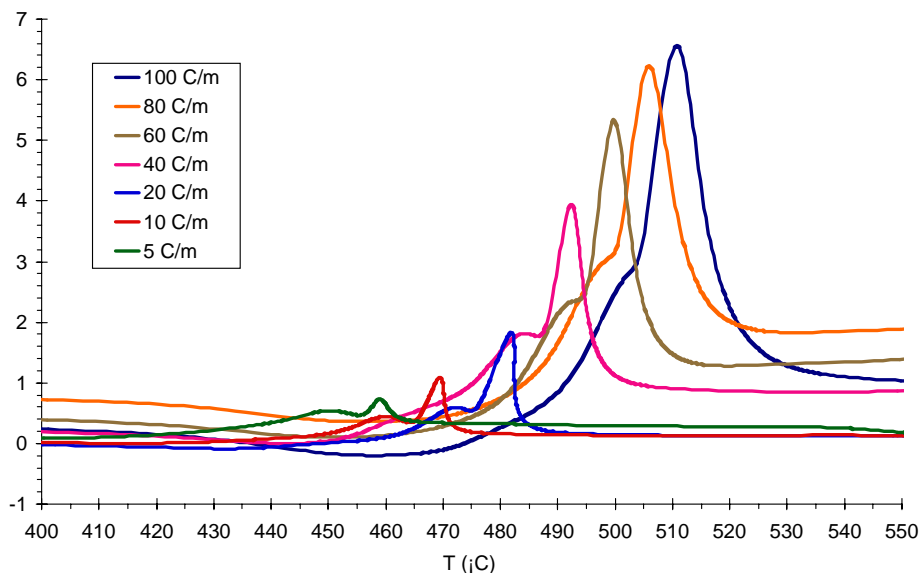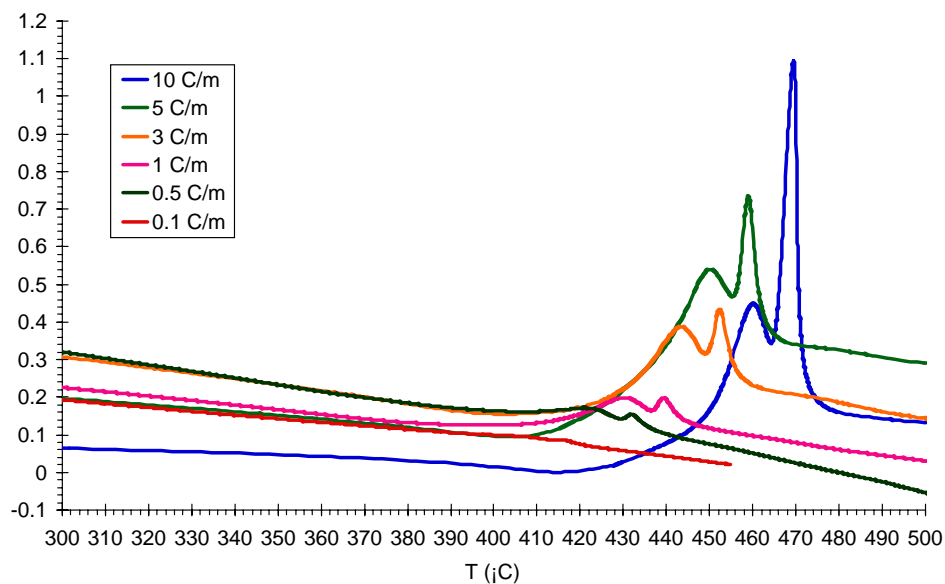
**Figure 8a,b**: Heating profiles obtained using Differential Scanning Calorimetry (DSC) for heating rates varying from 0.1°C/minute to 10°C/minute in (a), and from 5°C/minute to 100°C/minute in (b), illustrating the substantial effect of heating rate on the glass transition and crystallization response.

From Figures 8a and 8b, the following observations can be made.

(i)      The glass transition temperature and the onset of crystallization are shifted to higher temperatures with increasing heating rates, the effect being more pronounced in the lower heating rate regime spanning 0.1°C to 10°C per minute (Figure 8a).  This implies that precautions must be taken with regards to these kinetic effects when

18

isothermal heat treatments are conducted for understanding phase transformations and temperatures are selected based on DSC results conducted at 10°C/minute or 20°C/minute (which are the usual heating rates adopted in most research projects).

(ii)      Whereas at the lower heating rates, for example 3°C/minute or 5°C/minute (Figure 8a), a distinct double peak is observed during crystallization (as previously reported for this alloy—see Figure 1), with the first peak being interpreted as a phase separation peak [29], this is not as evident at the high heating rates where the first peak becomes a "shoulder" on the second peak (Figure 8b).  This implies that although both peaks shift to higher temperatures with increasing heating rate, the first peak shifts more than does the second peak.  Furthermore, the relative heights of the two peaks change with increasing heating rate, with the dominance of the first peak decreasing at progressively higher rates (compare data in Figures 8a and 8b).

The results from Figures 8a,b are summarized in Figure 9 where the three temperatures Tg, T1 and T2 are identified in the schematic DSC curve shown as an inset. It is evident that these three temperatures vary substantially with heating rate, the variation being more dramatic at the slow heating rates (up to ~10°C/minute) as alluded to above.  The second feature worth noting is that the difference between $T_g$ and T1 or T2 stays more or less constant for the different heating rates.

Until now it is implicitly assumed that the hydrogen distribution in the specimen is uniform since the samples were in the shape of thin disks of ~6 mm diameter and 0.2-0.5 mm thick.  A series of experiments were undertaken to verify this assumption.  These experiments were in part motivated by the cracking behavior following hydrogen charging of these disks for various times.  Cracks always initiated at the circumference and ran  radially inwards for a short distance before abruptly changing their propagation direction and running parallel to the circumference [27].
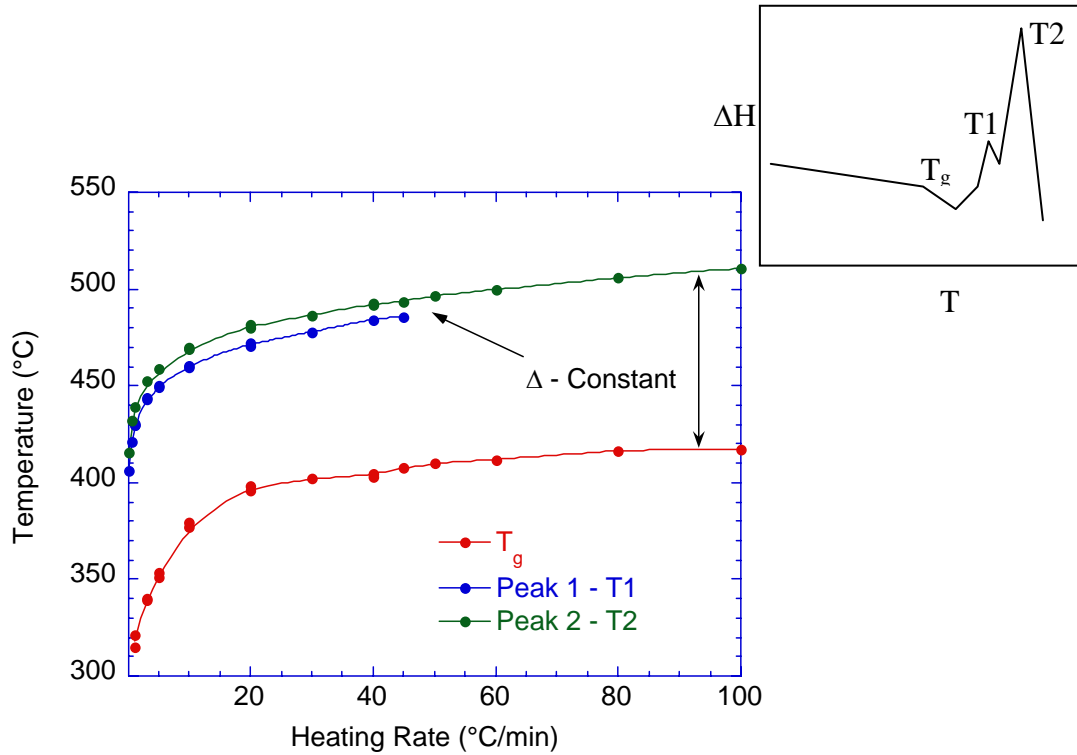
**Figure 9**: The variation in the glass transition temperature (Tg) and the crystallization response (as characterized by the peaks T1 and T2) with heating rate of BMG1.

Thus several disk specimens of BMG1 were sliced and charged for various lengths of time and the corresponding H/M in each instance was obtained. Such specimens were crushed into small pieces and DSC traces were obtained using a fixed heating rate. Next, duplicate specimens of those described above were obtained by charging for similar time intervals and measuring H/M from weight gain experiments. From these second set of specimens, the central 3-mm diameter region was cut out using a TEM specimen punch, leaving behind the outer annulus. The outer annulus thus obtained was then split into two pieces across the diameter. These individual pieces (the central 3-mm diameter piece and the two semi-circular annular pieces) were crushed and subjected to separate DSC heating runs. This enabled us to obtain DSC curves for the overall, as well as the outer region (in duplicate) and the inner region and determine whether there was a variation in response. Comparison of these outer and inner region curves for a specific charging time with those obtained for the overall specimen for different charging times permitted comparison of the response of the outer and inner regions. Examples from this exercise are shown in Figures 10 and 11.
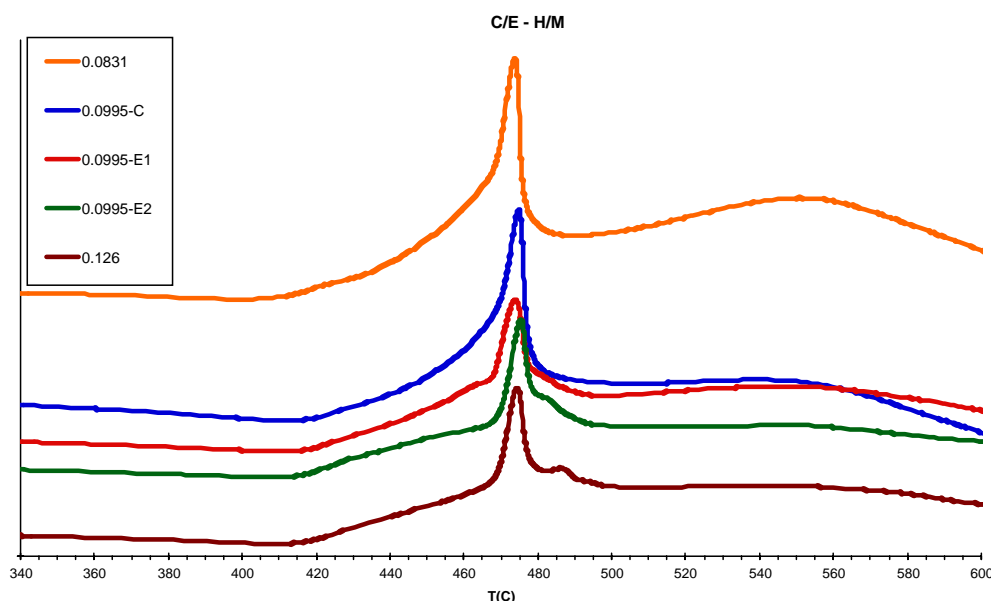
**Figure 10**: DSC response of hydrogen charged BMG1. The specimens were charged so that H/M was ~0.1. The uppermost curve and the lowest curve in the family of curves shown above are "average curves" and were obtained in each instance by crushing the entire charged specimen and subjecting it to a DSC scan. The H/M values were calculated to be 0.0831 and 0.126 respectively. In contrast, the family of three curves in between were obtained from a single specimen that was charged for a certain time and whose weight gain measurement indicated an H/M = 0.0995. The C, E1 and E2 in the legend represent "center" and "edge" (outer annulus) of the specimen as described in the previous paragraph.

An examination of the DSC traces in Figure 10 clearly demonstrates that the profiles for the center and edge are similar, and moreover virtually identical to the "average curves" for the specimens with H/M = 0.08 and 0.12. Thus, at this level of hydrogen charging (a fairly dilute level), it appears that hydrogen distribution in the specimen is fairly uniform. In contrast, in Figure 11 a set of DSC curves are shown for H/M ~0.3. The two upper curves in the figure correspond to average H/M values of 0.254 and 0.449. It is evident that these profiles are similar to each other but substantially different from the profiles observed for H/M of 0.1 in Figure 10. This is because hydrogen is not discharged during heating to any appreciable extent and instead interferes with the crystallization process, producing a complex set of hydrides [ 28-30]. The next three curves labeled 0.302-C, 0.302-E1 and 0.302-E2 correspond to the center and outer regions of a single specimen that was charged to an H/M level of 0.302. Clearly, the DSC response at the center is substantially different from that of the material

21

from the annulus.  The response at the center appears similar to the scans in Figure 10 whereas that of the annulus looks more like the profiles for the 0.254 or 0.449 material. Furthermore, the profile for 0.302-E1 and 0.302-E2 are similar, illustrating reproducibility.  Next, an altogether new specimen was charged to an H/M level of 0.327and the center and annulus regions were similarly scanned in the DSC.  These results are also included in Figure 11 (bottom two scans).  These scan are fully consistent with the observations made for the 0.302 specimen.
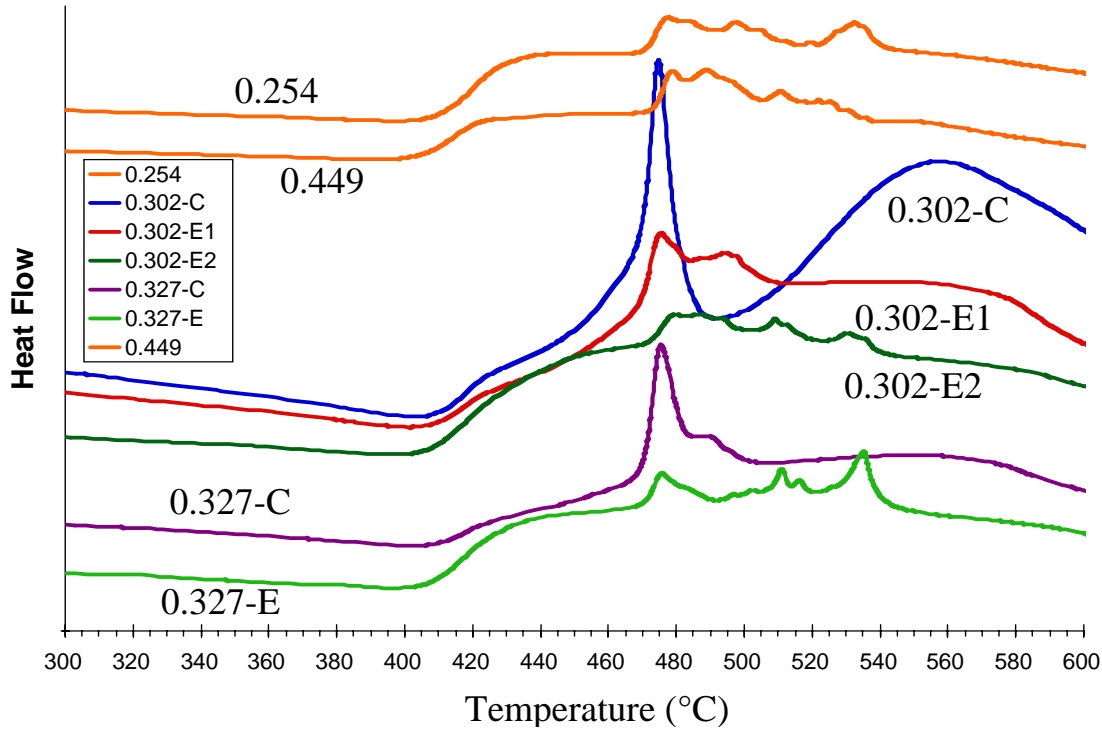


**Figure 11**:  DSC response of hydrogen charged BMG1.  The two uppermost curves are "average curves" for H/M = 0.254 and 0.449, obtained in each instance by crushing the entire charged specimen and subjecting it to a DSC scan.  (At these levels of H/M, there is enough hydrogen in the material to interfere with the crystallization process and the response is distinctly different from those observed for H/M = 0.1 in Figure 9).  Two sets of curves corresponding to nominal H/M values of 0.302 and 0.327 are also included where specimens from the center and the annulus were scanned. The C, E1 and E2 in the legend represent "center" and "edge" (outer annulus) of the specimen.

These results suggest that hydrogen distribution in the specimen is non-uniform when hydrogen charging is such that the overall H/M value is moderately high.. A comparison of Figures 10 and 11 indicates that the center saturates at a low hydrogen level (H/M ~ 0.1) whereas the outside can take in more hydrogen.  Similar effects were also observed at H/M = 0.5.

Since the specimen surface and geometry were such that all regions were equally efficiently exposed to the electrolyte and hence hydrogen intake, we do not know whether what is observed is a kinetic effect (or an equilibrium solubility effect) arising as a consequence of structural differences between the center and the periphery. The origin of the structural difference could be mechanical stress or chemical (arising from gradients in cooling rate from the outside to the center during solidification), or both. It was previously shown that an intermediate anneal at a temperature well below the glass transition temperature leads to a reduced rate of hydrogen intake during charging [27].

## 4.4    Gas Charging of BMG1, BMG3 and BMG4

Three of the compositions (BMG1, BMG3 and BMG4) were subjected to gas charging of hydrogen under pressure, and the hydrogenation kinetics was examined. For this, as previously mentioned, specimens were shipped to Dr. John Vajo of HRL Laboratories in Malibu, CA. The samples were pulverized and placed in a Sieverts apparatus and subjected to 100 atmospheres of hydrogen and heated upto 400°C. Specimens were either held at this temperature or immediately cooled down to room temperature. Next, the specimen was heated back up to the same temperature in vacuum to desorb the hydrogen. This entire step then represented a single cycle of hydrogenation-dehydrogenation. The desorption experiment was not conducted on BMG3 and BMG4. In the case of BMG1, a second cycle was also performed. The hydrogen intake and output were monitored by weight change measurements. Results for each of the three materials follow:

**BMG1** (52.5Zr-17.9Cu-14.6Ni-5.0Ti-10.0Al):

The results of the gas charging experiments for BMG1 are summarized in Figure 12a. The temperature profile against time representing the heating rate is shown and the right vertical axis presents temperature, whereas the left vertical axis presents hydrogen intake and output. *In the first hydrogenation cycle*, the temperature was raised at a constant
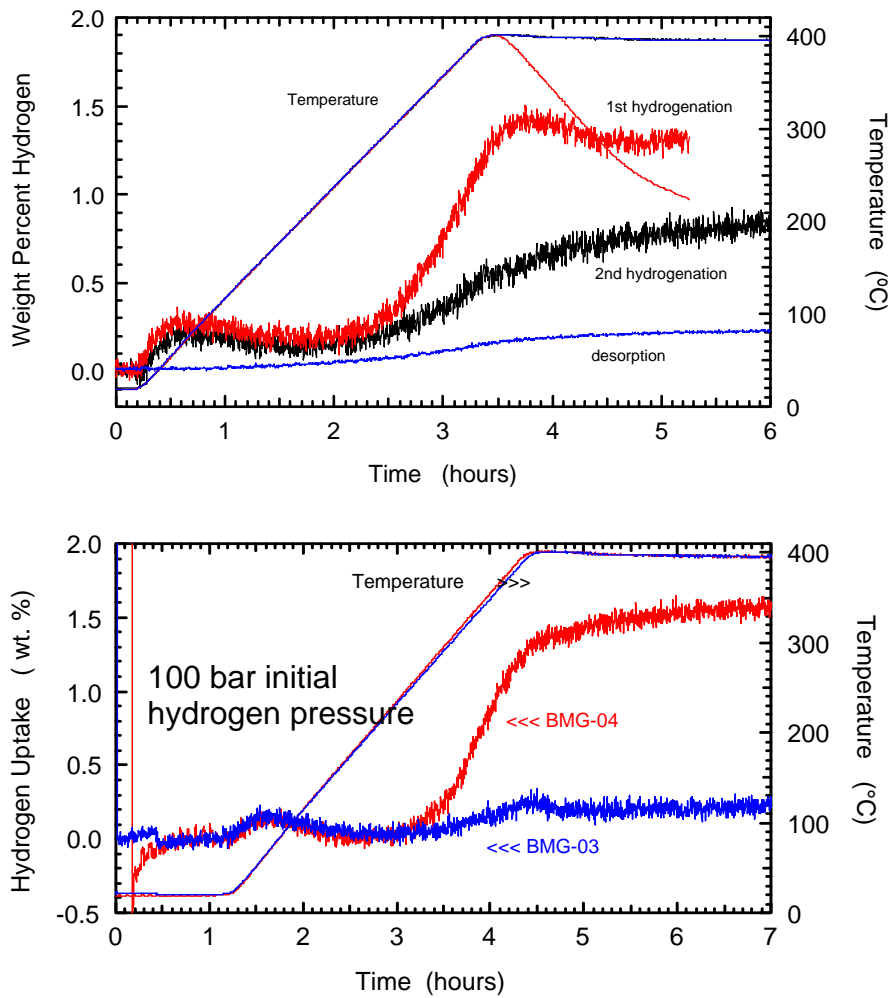
23

**Figure 12**: Gas charging in a 100 atmosphere hydrogen pressure in a modified Sievert's apparatus as a function of temperature (a) BMG1: charging, discharging and recharging, and (b) BMG3 and BMG4: single cycle charging only.

heating rate to 400°C (blue line) and then the specimen was cooled down immediately (red line) so that the residence time at 400°C was negligible. The hydrogen intake during heat up is a maximum between 100°C and 400°C but since there was no hold time at 400°C, saturation is not accomplished, and during the cool down, there is no further hydrogen intake as depicted by the plateau in the red curve (corresponding to the time segment where the temperature was decreased from 400°C to room temperature). The total hydrogen intake during the first heat up is ~1.4-1.5 wt.% hydrogen. Attempts to subsequently desorb the hydrogen by heating in vacuum demonstrated that only a small amount of hydrogen (~0.2 wt%) is given up (blue desorption curve). *A second hydrogenation cycle* by heating to 400°C and holding a temperature (blue temperature profile) demonstrated that it was possible to put more hydrogen into the material (black curve) which then ultimately reaches a plateau level of 0.6-0.7 wt.% hydrogen, so that a

total hydrogen level of ~2 wt.% has been incorporated into the alloy. This approximately corresponds to and H/M = 1.5, which is in good agreement with that obtained as the saturation value by electrochemical charging (Figure Y reproduced from Reference [27]).

**BMG3** (Fe (54-55)-Mn (10)-Cr (4)-Mo (10)-C (15)-B (6-7))

Gas charging of BMG3 illustrated that its hydrogen absorption capacity is minimal (blue curve in Figure 12b) in the temperature range 20°C-400°C at a pressure of 100 atmospheres. This observation is consistent with electrochemical charging results where the specimen repeatedly fractured on charging at immeasurable weight gain levels. The inability to ingest hydrogen may result from the fact that this alloy contains a high level of carbon and boron, both of which are "small" atoms that effectively reduces the size of the interstices that are potential hydrogen sites.

**BMG4** (Cu (47)-Ti (34)-Zr (11)-Ni (8) – Vitralloy 101)

As discussed earlier, the DSC results for this alloy was not in agreement with results reported in the literature for an alloy of similar composition even though our results were reproducible. This has raised questions regarding this specific composition. Attempts to procure additional material were futile. Gas charging was however performed on the available material and the results are included in Figure12b. It is evident from this figure that it is possible to gas charge this material to the level of ~1.6 wt.% hydrogen at 400°C with the maximum hydrogen uptake occurring between 150°C and 250°C. Holding the alloy at 400°C for a period of time in a hydrogen environment of 100 atmospheres indicates that saturation is reached. Due to time constraints at HRL Laboratories, dehydrogenation experiments were not conducted on this alloy, but it is suggested that the reduced level of Ti and Zr in this alloy may permit hydrogen removal more readily than in BMG1.

(a) Papers published in peer-reviewed journals
        None

(b) Papers published in non-peer-reviewed journals or in conference proceedings
        None

(c) Papers presented at meetings, but not published in conference proceedings
        "Hydrogen charging of a Zr-based Bulk metallic Glass", P. Wang and
        K.S. Kumar, TMS Annual Meeting in Charlotte, NC., March 14-18, 2004.

(d) Manuscripts submitted, but not published
        None

(e) Technical reports submitted to ARO
        "Hydrogen in Bulk metallic Glasses: Storage Potential and its Effects on
        Structure", by K. Sharvan Kumar, Interim Progress Report, submitted
        May 2003.


## 6.0     List of Participating Scientific Personnel

K. Sharvan Kumar – Principal Investigator
Ping Wang – Post-Doctoral Research Associate

## 7.0     Report of Inventions

None

# 8.0    Bibliography

1.    L. Schlapbach, MRS Bulletin, 27(9), September 2002, pp.675-676.
2.    J.J. Reilly, *Zeitschrift fur Physikalische Chemie Neue Folge* 117, 655 (1979).
3.    Z.S. Wronski, *International Materials Reviews*, 46, 1 (2001).
4.    "Hydrogen Sotrage", in the MRS Bulletin, Volume 27, No.9, September 2002, Materials Research Society, Warrendale, PA. pp 675-712.
5.    H.W. Schroeder, "Hydrogen in Zr-based Metallic Glasses", in <u>Rapidly Quenched Metals</u>, editors: S. Steeb and H. Warlimont, Elsevier Science, 1985, p. 1525.
6.    F.H.M. Spit, J.W. Drijver and S. Radelaar, *Scripta Metallurgica*, 14, 1071 (1980).
7.    F.H.M. Spit, J.W. Drijver and S. Radelaar, in *Zeitschrift fur Physikalische Chemie Neue Folge* 116, 225 (1979).
8.    A.J. Maeland, "Hydrogen in Crystalline and Non-Crystalline Metals and Alloys: Similarities and Differences", in <u>Rapidly Quenched</u> <u>Metals</u>, editors: S. Steeb and H. Warlimont, Elsevier Science, 1985, p. 1507.
9.    A.J. Maeland, L.E. Tanner, and G.G. Libowitz, *Journal of the Less-Common Metals*, 74, 279 (1980).
10.   R. Kirchheim, F. Sommer and G. Schluckebier, *Acta Metallurgica*, 30, 1059 (1982).
11.   J.M. Riveiro and B. Seoane, *Journal of Non-Crystalline Solids*, 163, 315 (1993).
12.   J.H. Harris, W.A. Curitn, and M.A. Tenhover, *Physical Review B*, 36, 5784 (1987).
13.   S. Yamaura, K. Isogai, H. Kimura, and A. Inoue, *Journal of Materials Research*, 17, 60 (2002).
14.   D. Zander, H. Leptien, U. Koster, N. Eliaz and D. Eliezer, *Journal of Non-Crystalline Solids*, 250-252, 893 (1999).
15.   D. Zander and U. Koster, *Materials Science and Engineering*, A304-306, 292 (2001).
16.   N. Eliaz, D. Eliezer, E. Abramov, D. Zander and U. Koster, *Journal of Alloys and Compounds*, 305, 272 (2000).
17.   U. Koster, D. Zander, Triwikantoro, A. Rudiger and L. Jastrow, *Scripta Materialia*, 44, 1649 (2001).
18.   J.H. Harris, W.A. Curtin and L. Schultz, *Journal of Materials Research*, 3, 872 (1988).
19.   D. Zander, U. Koster, and V. Khare, Materials Research Society Symposium Proceedings, Vol. 643, 2001, pp. K2.2.1-K2.2.6
20.   A. Inoue, T. Zhang, K. Ohba and T. Shibata, *Mater. Trans. JIM*, **36**, 876 (1995).
21.   T. Shoji and A. Inoue, *Journal of Alloys and Compounds*, 292, 275 (1999).
22.   R.B. Schwartz, *MRS Bulletin*, November 1999, pp. 40-43.
23.   S.-I. Yamaura, K. Isogai, H. Kimura and A. Inoue, *Jour. Mater. Res.*, 17, 60 (2002).
24.   S.J. Pang, T. Zhang, K. Asami and A. Inoue, *Acta Materialia*, 50, 489 (2002).
25.   A. Inoue, *Acta Materialia*, 48, 279 (2000).
26.   F.Q. Guo, S.J. Enouf, S.J. Poon and G.J. Shiflet, *Philos. Mag. Lett.*, 81, 203 (2001).
27.   K.S. Kumar, "Zr-based Bulk metallic Glasses for Hydrogen Storage" – Final Report on Contract # MDA972-01-1-0034. Submitted to DARPA, April 18, 2003.

28. N. Eliaz, D. Eliezer, E. Abramov, D. Zander and U. Koster, *Journal of Alloys and Compounds*, 305, 272 (2000).
29. D. Suh and R. H. Dauskardt, *Mater. Sci. Eng.*, A319-321, 480 (2001).
30. N. Ismail, A. Gerbert, M. Uhlemann, J. Eckert and L. Schultz, *Journal of Alloys and Compounds*, 314, 170 (2001).
31. X.H. Lin and W.L. Johnson, *Jour. Appl. Phys.*, 78, 6514 (1995).
32. S.C. Glade, J.F. Loffler, S. Bossuyt and W.L. Johnson, *Jour. Appl. Phys.*, 89, 1573 (2001).
33. W.L. Johnson, private communications.